Letter to the Editor

Preoperative considerations of inflammation and metastasis in cardiac malignancies: a description of two cases

Shangwei Ding[1#], Juanmei Chen[1,2#], Xuenian Huang[1], Caiqin Zheng[1], Ting Sun[1], Zelin Wu[3], Jilong Qin[4]

[1]Department of Ultrasound, the First Affiliated Hospital of Guangzhou Medical University, Guangzhou, China; [2]The Second Clinical Medicine School of Guangzhou Medical University, Guangzhou, China; [3]Department of Pediatrics, the First Affiliated Hospital of Guangzhou Medical University, Guangzhou, China; [4]Department of Pathology, the First Affiliated Hospital of Guangzhou Medical University, Guangzhou, China

[#]These authors contributed equally to this work and should be considered as co-first authors.

Correspondence to: Jilong Qin. Department of Pathology, the First Affiliated Hospital of Guangzhou Medical University, No. 151, Yanjiang West Road, Yuexiu District, Guangzhou 510120, China. Email: 2753927067@qq.com.

Submitted Sep 21, 2022. Accepted for publication Mar 05, 2023. Published online Mar 30, 2023.
doi: 10.21037/qims-22-1002
View this article at: https://dx.doi.org/10.21037/qims-22-1002

Introduction

Primary cardiac tumors (PCTs) are rare, with an incidence ranging from 0.001% to 0.030% at autopsy. A quarter of PCTs are malignant, and most are sarcomas and thus prone to early hematogenous metastases (1). A literature review analyzed the histological types of 72 cases of PCT after surgery and found that the most common cardiac tumor was myxoma in 49 cases (68%), followed by papillary fibroelastoma in 13 cases (18%) and sarcoma in 6 cases (8.3%) (2). Another study in a tertiary referral center showed that primary cardiac angiosarcoma (PCAS) mainly occurred in the right atrium, and 56% of patients with PCAS in this center developed metastatic disease and lung or pleural metastases (3). Due to the particular growth position of the primary cardiac malignancies, partial tumor tissue cannot be resected with clear margins, and there may be recurrence after surgery. Malignancies are highly aggressive and prone to early metastasis. Some cardiac malignancies may have already metastasized before surgery with no metastases detected on imaging. Clinicians may ignore possible metastases and simply remove the initial primary tumor. For all these reasons patients with primary cardiac malignancies tend to have a poor prognosis.

Unlike for other organ tumors, it is difficult to obtain biopsies, such as endomyocardial biopsy (EMB), from cardiac tumors that have severe tissue trauma and serious complications (4). Clinicians may not be able to perform histopathological detection through minimally invasive biopsy to determine the pathological type of the tumor and formulate a detailed and safe surgical plan. Therefore, cardiac imaging may be useful in the diagnosis of cardiac tumors.

Inflammation is the defensive response of living tissues in the vascular system to damaging factors. There are many causes of inflammation, including infections, autoimmune diseases, cancer, and chemical exposure. Long-term inflammation may cause cancer (5). Cancer-related inflammation (CRI) is characterized by the presence of inflammatory cells and inflammatory mediators in tumor tissue, with tissue remodeling, repair, and angiogenesis being similar to chronic inflammatory responses (6). CRI, as a metastasis-promoting factor and can enhance the aggressiveness of cancer (7). Although imaging can identify metastases with obvious morphological features, it is difficult to identify inflammation and early metastases. Furthermore, the absence of tumor lesions on imaging does not mean the metastases, such as micrometastases, do not exist. Recently, we encountered 2 similar cases that highlight the importance of considering malignancy as the underlying cause of pneumonia of unclear etiology.

Case presentation

All procedures performed in this study were conducted in accordance with the Declaration of Helsinki (as revised in

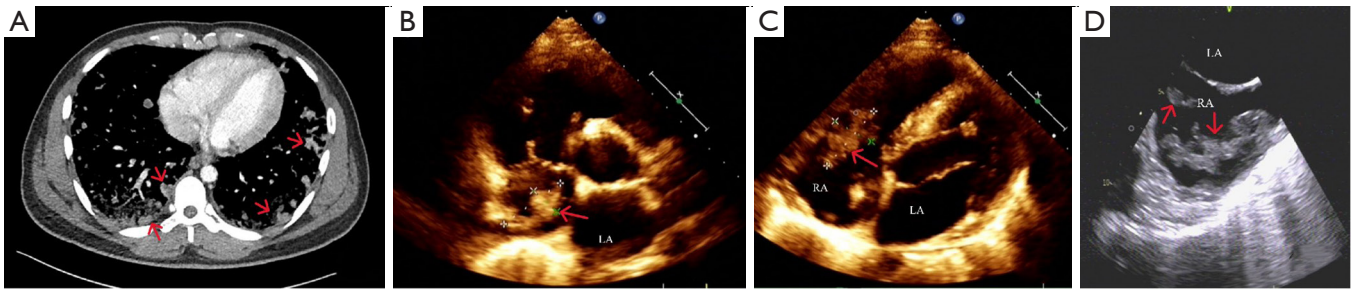

Figure 1 The patient's images. (A) Thoracic CT showed multiple polymorphic lesions in the bilateral lungs. Vasculitic lesions or hematogenous lung infection were considered, and there was alveolar hemorrhage in bilateral lungs (arrows). (B,C) TTE showed an enlargement of vegetation on the tricuspid valve (B, arrow) and a new neoplasm at the entrance to the inferior vena cava (C, arrow). (D) TEE showed vegetation to the right auricle without adhesion to the tricuspid valve. The size was 68 mm × 29 mm (arrows). LA, left atrium; RA, right atrium; CT, computed tomography; TTE, transthoracic echocardiography; TEE, transesophageal echocardiography.

2013) and with the ethical standards of Ethics Committee at The First Affiliated Hospital of Guangzhou Medical University. Written informed consent was obtained from the patient or the patient's parents to publish this case report and accompanying images. A copy of the written consent is available for review by the editorial office of this journal.

Case 1 was a 23-year-old man who had a cough and hemoptysis for more than 4 weeks and was admitted to the hospital with a fever, which he had for 3 days. Chest computed tomography (CT) (September 4, 2019) from 2 weeks earlier showed diffuse multiple small nodules with patchy peripheral opacities in bilateral lungs. Tuberculosis was excluded based on the examination at the chest hospital. Echocardiography showed moderate regurgitation of the tricuspid valve and an abnormal echo on the tricuspid valve, suggesting possible tricuspid chordae rupture. One week prior to admission, he was hospitalized in another hospital, where echocardiography (September 11, 2019) showed an abnormal echo mass (thrombosis or a tumor) in the right atrium, and 3 sequences of saccharomycetes were detected in the blood by the Beijing Genomics Institution (BGI). It was diagnosed as "lung fungal infection, right atrial thrombosis", and antifungal drugs, such as caspofungin acetate and voriconazole, were administered. The effect was not good, and the patient still had a cough and hemoptysis.

Three days prior to admission to our hospital, the patient developed a fever, and his temperature was 38.3–38.8 ℃. A review of the chest CT (September 17, 2019) showed diffuse multimorbidity in bilateral lungs, with rapidly progressing lesions, which were considered diffuse alveolar hemorrhage with vasculitis. Thrombosis in the right atrial was possible. In order to seek further diagnosis and treatment, he was transferred to the First Affiliated Hospital of Guangzhou Medical University (September 18, 2019). His vital signs at admission were as follows: temperature, 36.9 ℃; heart rate, 123 bpm; breath, 23 bpm; blood pressure, 114/60 mmHg; oxygen saturation (SPO_2), 81%; and bilateral lower lung auscultation with crackles. The white blood cell (WBC) count was 10.5×10^9/L, the C-reactive protein (CRP) level was 2.14 mg/dL, and his hemoglobin (Hb) level was 50 g/L. The results of chest enhancement CT and 3-dimensional reconstruction (September 19, 2019) showed multiple polymorphic lesions in bilateral lungs, suggestive of vasculitic lesions or hematogenous lung infection may be possible, and alveolar hemorrhage in bilateral lungs (*Figure 1A*). The patient also had a right atrial filling defect (vegetation or thrombosis) and multiple slightly low-density nodules in the liver suggestive of hematogenous intrahepatic infection. Based on the results of relevant examinations, the possibility of a hematogenous disseminated lung abscess was considered. Vancomycin and meropenem were administered to counter the infection, and voriconazole was administered for antifungal treatment. The liver ultrasound and contrast ultrasonography (September 20, 2019) showed that intrahepatic lesions were benign (infectious lesions may be possible). The transthoracic echocardiography (TTE; September 19, 2019) review revealed an enlargement of vegetation on the tricuspid valve (*Figure 1B*) and a new neoplasm at the entrance to the inferior vena cava (*Figure 1C*). Transesophageal echocardiography (TEE; September 24, 2019) further found vegetation to the right auricle without adhesion to the tricuspid valve, with a size of 68 mm × 29 mm (*Figure 1D*). During hospitalization,

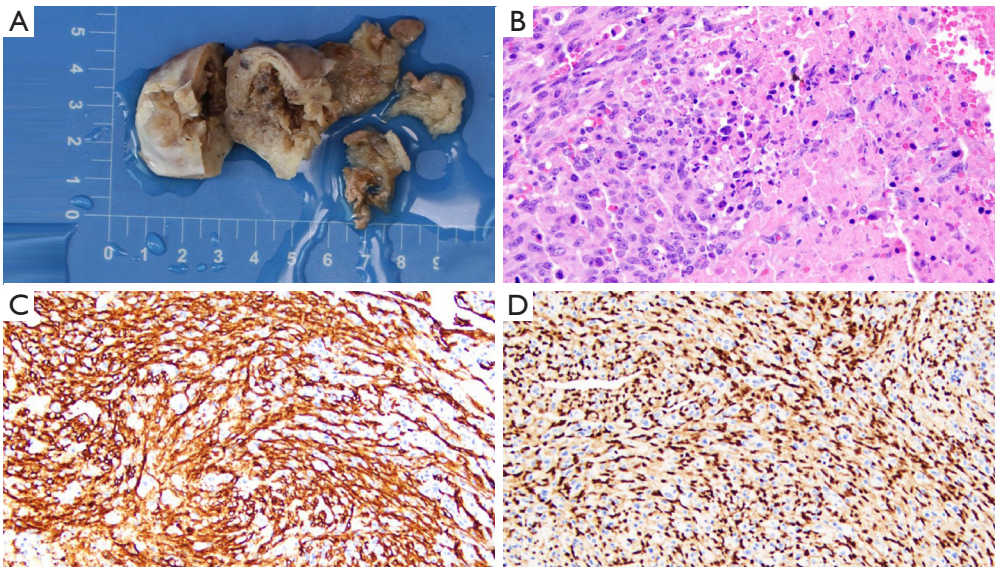

Figure 2 The pathological results of the tumor identified vascular malignancies (angiosarcoma). (A) The tumor in the right atrium was about 60 mm × 50 mm in size. (B) HE staining at ×200. Most cells were atypical, abundant short fusiform, and ovoid cells arranged in bundles. (C,D) Immunohistochemical stain. (C) CD31(+) ×200. (D) ERG(+) ×200. HE, hematoxylin and eosin; ERG, ETS related gene; ETS, erythroblast transformation specific.

multiple bacterial and fungal blood cultures were negative.

During a week of antifungal and antibacterial treatment, the patient's symptoms did not improve significantly. Multiple infectious lesions in the lung and liver were thought to be caused by hematogenous disseminated infections that originated from macrovegetations in the heart. In the absence of an effective means to control the infection, after consultation and evaluation of cardiac surgeons, it was considered that the vegetation in the heart could be removed surgically to improve the infection and bleeding in the lungs. After thorough preparation, the surgery was performed on September 27, 2019. During the operation, a tumor was found in the right atrium, about 60 mm ×50 mm in size, which had invaded the atrial tissue. The mass was completely removed by the surgeon (*Figure 2A*). After surgery, endotracheal intubation and assisted ventilation were implemented, antifungal drugs were discontinued, and anti-infective therapy continued with vancomycin and meropenem. The patient's vital signs were stable and SPO_2 was 100%, but multiple bedside chest radiographs showed no significant changes in the bilateral lungs.

On the seventh postoperative day, the endotracheal tube was removed, and assisted ventilation continued. Fourteen days after surgery, the pathological results confirmed that the patient had a malignant vascular tumor (angiosarcoma; *Figure 2B-2D*). The doctor explained the condition to the patient and his family, and it was indicated that the patient's intrapulmonary and intrahepatic lesions might be tumors and that the prognosis was poor. The patient had difficulty breathing and refused endotracheal intubation soon after, and the family also decided to halt treatment when he was in critical condition. The patient's dyspnea worsened the next day, SPO_2 was 70% under pure oxygen conditions, and the SPO_2 continued to drop to 30% after endotracheal intubation. The patient became comatose and died.

Case 2 was a 7-year-old girl treated in another hospital due to dull pain and discomfort in the left lumbar and abdomen for more than a month. The chest and abdominal CT examination showed multiple mass lesions in bilateral lungs and mediastinum, and left iliopsoas parapsoas. In order to further clarify the diagnosis and treatment, she was transferred to our hospital. The CT review suggested metastases in the left lower lung hilum associated with peripheral inflammatory exudation (*Figure 3A*), with possible pleural metastases in the lower right lung. WBC was 6.56×10^9/L and CRP was 0.94 mg/dL. A routine abdominal ultrasound showed a solid mass in the left lower abdominal sac, but contrast-enhanced ultrasound (CEUS) suggested it was not malignant. A lymphangial cyst was

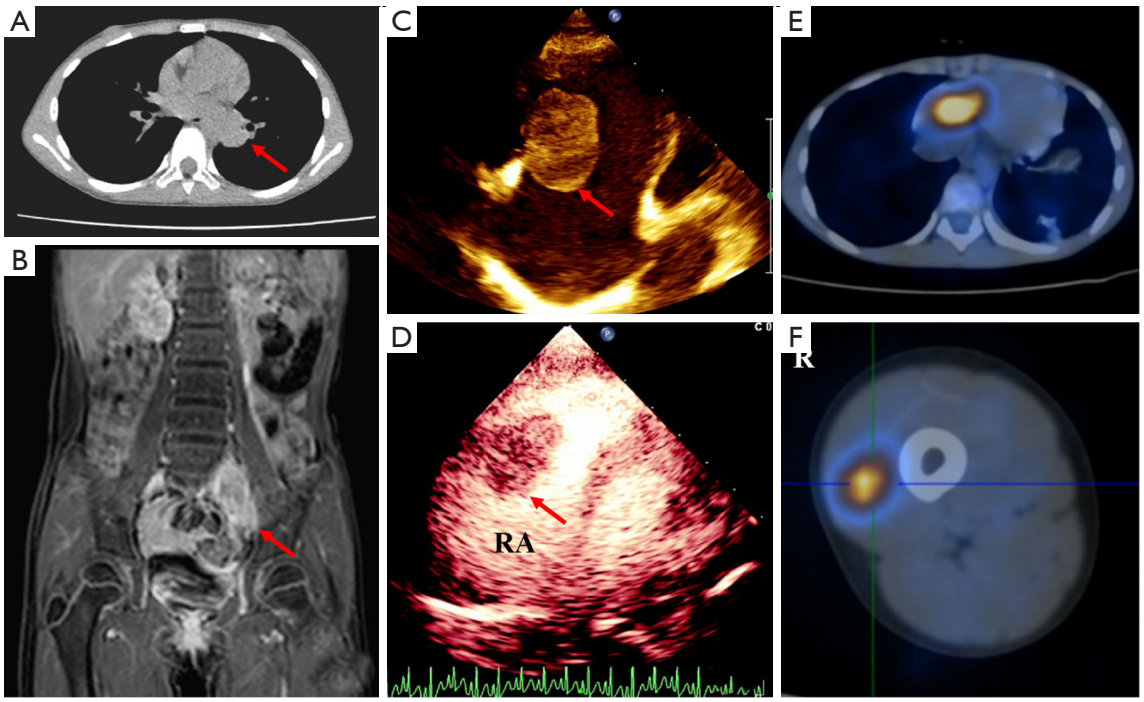

Figure 3 The patient's images. (A) CT review suggested metastases in the left lower lung hilum associated with peripheral inflammation (arrow). (B) The abdomen MRI showed a mass near the left iliac vessels (arrow). (C) TTE showed a solid mass in the right atrium (27 mm × 22 mm; arrow). (D) CE revealed abundant blood flow in the tumor (arrow). (E,F) PET-CT showed a hypermetabolic nodule (SUV 9.7) at the junction of the right atrium and right ventricle (E) and a hypermetabolic nodule (SUV 6.7) between the medial thigh muscle and the lateral thigh muscle of the right thigh (F). RA, right atrium; CT, computed tomography; MRI, magnetic resonance imaging; TTE, transthoracic echocardiography; CE, contrast echocardiography; PET-CT, positron emission tomography-computed tomography; SUV, standard uptake value.

considered. Magnetic resonance imaging (MRI) of the abdomen showed a mass near the left iliac vessels (*Figure 3B*) and a nodular shadow between the left gluteus maximus and gluteus mesomus. Lymphoma or lymphadenopathy were suspected. Therefore, laparoscopic abdominal mass biopsy and left inguinal lymph node biopsy were arranged for the patient. The pathological results identified lymph node proliferative changes but no tumor cells. Mycobacterium tuberculosis nucleic acid tests were also performed to exclude tuberculosis, and the results were negative. The patient's abdominal pain was less severe than that before anti-infective therapy with cefixime, and she was discharged.

Two months later, the girl returned to our hospital. She had developed intermittent left leg pain and a cough for about 1 month, accompanied by hemoptysis for 5 days. Routine TTE showed a solid mass in the right atrium (27 mm × 22 mm) that had high mobility and was lobulated, and it was considered a malignant lesion (*Figure 3C*). The CT review suggested pleural metastasis in the right lower lung, so an ultrasound-guided biopsy with a 20-G biopsy gun (BARD® MAGNUM®) was performed on the pleura. However, the pathological finding was also infectious disease. To explore the nature of the atrial mass, further contrast echocardiography (CE) was performed, revealing a very rich blood supply within the mass. The perfusion intensity and time were similar to those of the myocardium, and there was no necrosis. The mass was diagnosed as a malignant tumor (*Figure 3D*). Then, positron emission tomography (PET)-CT was used to determine whether there were metastases throughout the body, and clear positive results were obtained. The right atrial mass was a primary cardiac malignancy (*Figure 3E*), and there was a metastasis between the muscles of the right middle thigh (*Figure 3F*). Ultrasound-guided biopsy with a 20-G biopsy gun (BARD® MAGNUM®) for the mass in the right thigh was performed, and the pathological result was

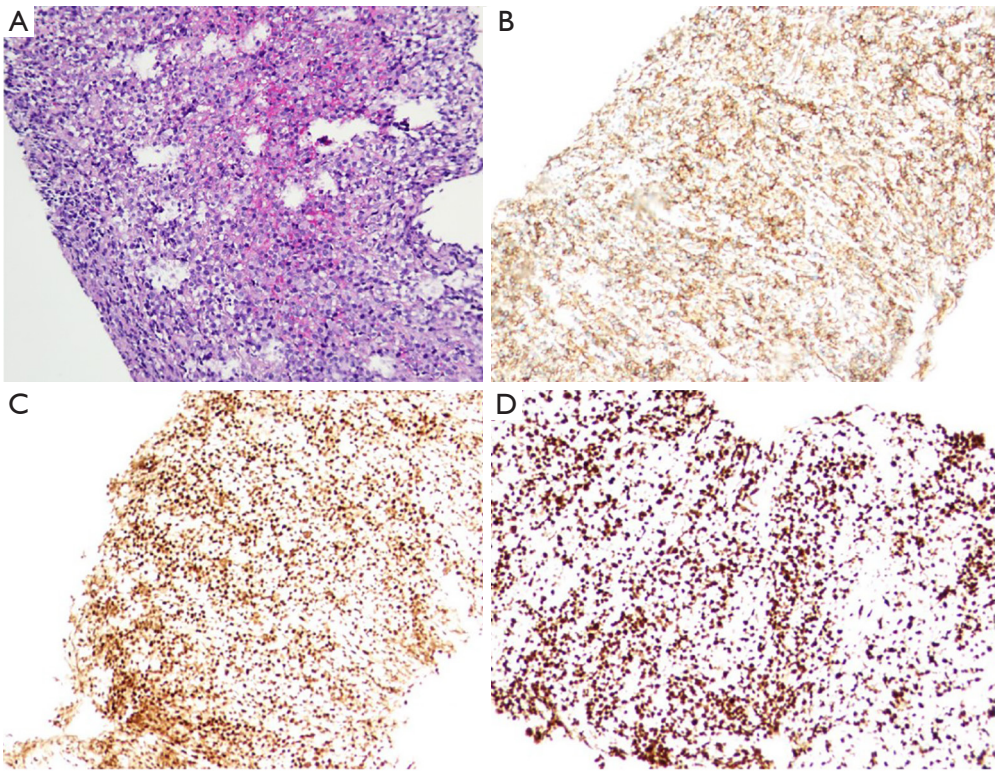

Figure 4 The pathological result of the right thigh tumor was Ewing sarcoma. (A) HE staining at ×200. (B-D) Immunohistochemical staining. (B) CD99(+) ×100. (C) FLi1(+) ×100. (D) Ki67(+) ×100. HE, hematoxylin and eosin. FLi1, Friend leukemia integration-1.

Ewing sarcoma (*Figure 4A-4D*). A vindesine, ifosfamide, doxorubicin, and etoposide (VIDE) chemotherapy regimen was then used for the patient.

After 2 rounds of chemotherapy, the cardiac tumor was significantly smaller than before, pulmonary lesions had reduced significantly, and the mass in the right thigh had disappeared (*Table 1*). After the fifth round of chemotherapy, PET-CT showed no hypermetabolic tissue in the right thigh or right atrium (*Figure 5A,5B*). TTE still detected abnormal masses near the right atrial appendage, and the size was stable (*Figure 5C*). After 6 rounds of VIDE chemotherapy, the regimen was changed to vincristine, irinotecan, and temozolomide (VIT) chemotherapy, but no obvious changes were detected in TEE and PET-CT over the next 6 VIT chemotherapy sessions. Then, the girl stopped the chemotherapy and was followed up by TTE. About half a year later, TTE showed no obvious change in the size of the right atrial mass, but a new cord-like attachment was identified on the mass surface, which wiggled with the heartbeat (*Figure 5D*). The cord-like attachment did not increase or disappear during the follow-up, and its nature remained unclear.

Discussion

The 2 cases final diagnoses were cardiac malignancy, 1 with PCAS and the other with Ewing sarcoma. The first patient's malignancy was masked by severe pneumonia, leading to an erroneous diagnosis of infective endocarditis. The second patient's cardiac malignancy was treated by actively obtaining the pathological tissue of the tumor and then the initiation of targeted chemotherapy. In these 2 cases, both patients presented with a fever and pulmonary symptoms. The characteristics of inflammation in the lung and other organs were the main reason for the initial misleading diagnosis, and the effect of anti-inflammatory treatment was not good. The first patient was seriously ill, with severe pneumonia and serious impairment of pulmonary function. However, in case 2, the pneumonia was mild, and the basic state of the patient was good. Multiple biopsies were performed to obtain the correct pathological diagnosis in case 2, and the patient received chemotherapy and

Table 1 Timeline of condition change of case 2

Time	Event	Result
Other hospital: (chief complaint: fever and dull pain in left waist and abdomen)		
May 12, 2020	CT	Multiple occupancies of bilateral lungs, soft-tissue mass adjacent to left iliopsoas muscle
Our hospital (first hospitalization): transferred to our hospital for further treatment		
May 15, 2020	Thoracic CT review (*Figure 3A*)	High probability of left lower lung hilum malignant lesions, bilateral lungs, and right pleural metastasis
May 18, 2020	Abdominal CEUS	Left lower abdominal mass: lymphangial cyst
May 19, 2020	Abdominal MRI	Lymphadenopathy
May 22, 2020	Lymph node biopsy	Pathology: reactive hyperplastic changes, no tumor
May 26, 2020	Thoracic MRI	Left hilar mass: lymph node tuberculosis Slight inflammation of the left lower lung
June 1, 2020	Discharge	Abdominal pain was less severe than before
Our hospital (second hospitalization): intermittent left leg pain, cough, and hemoptysis occurred		
July 24, 2020	Thoracic CT	Multiple lesions were added in the lungs: infection was considered likely
July 29, 2020	TTE (*Figure 3C*)	Right atrial mass (27 mm × 22 mm), angiosarcoma?
August 5, 2020	Pleural biopsy	Infective lesion
August 6, 2020	CE (*Figure 3D*)	Rich blood supply, considered a malignant tumor
August 6, 2020	PET-CT (*Figure 3E,3F*)	Primary cardiac malignancy; high metabolic nodular of the right thigh, considered metastases; lung infection
August 12, 2020	Right thigh biopsy	Pathology: Ewing sarcoma
VIDE chemotherapy (August 24, 2020, December 22, 2020: first round of chemotherapy to sixth round of chemotherapy)		
September 9, 2020	TTE	The tumor reduced significantly (17 mm × 12 mm)
September 17, 2020	MRI	The mass of the right thigh had almost disappeared
November 27, 2020	PET-CT (*Figure 5A,5B*)	Glycometabolism of right thigh and RA decreased to the background level
November 30, 2020	TTE (*Figure 5C*)	RA tumor size (15 mm × 11 mm)
VIT chemotherapy (January 26, 2021, May 6, 2021: first round of chemotherapy to sixth round of chemotherapy)		
March 8, 2021	TTE	RA tumor size (12 mm × 11 mm)
March 15, 2021	PET-CT	No increased glycometabolism in the right thigh and RA
May 7, 2021	TTE	Tumor size was stable; normal heart tissue
Follow-up		
October 26, 2021	TTE (*Figure 5D*)	Tumor size was 11 mm × 10 mm; the surface of the tumor is newly reborn cord-like tissue
November 11, 2021, to August 14, 2022	Multiple TTE	No significant change in tumor size; no increase or disappearance of surface attachment cord-like tissue

CT, computed tomography; CEUS, contrast-enhanced ultrasound; MRI, magnetic resonance imaging; TTE, transthoracic echocardiography; CE, contrast echocardiography; PET-CT, positron emission tomography-computed tomography; VIDE, vindesine, ifosfamide, doxorubicin, etoposide; RA, right atrium; VIT, vincristine, irinotecan, temozolomide.

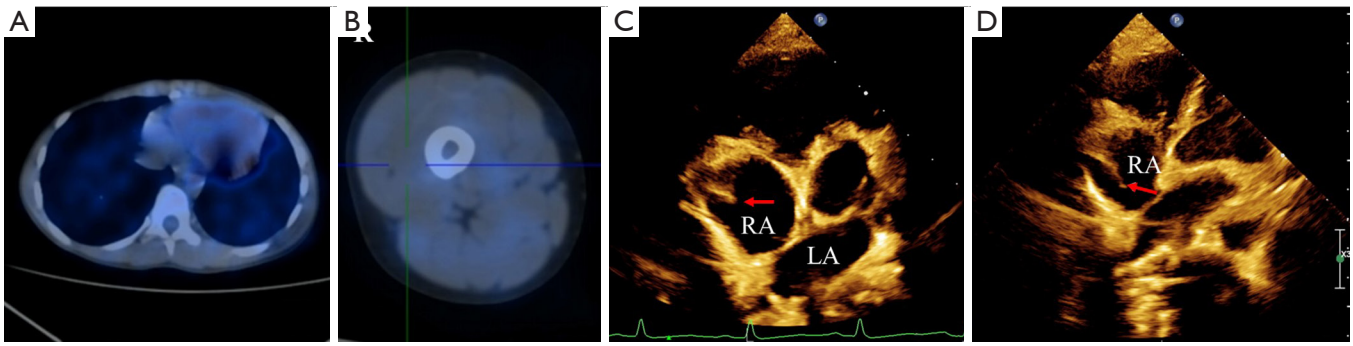

Figure 5 The patient's images. (A,B) PET-CT showed no abnormal glycometabolism in the right atrium (A) and the right thigh (B) after the fifth round of VIDE chemotherapy. (C) TTE showed abnormal masses near the right atrial appendage (arrow). (D) TTE showed a cord-like attachment on the mass surface that wiggled with the heartbeat at the follow-up (arrow). RA, right atrium; LA, left atrium; PET-CT, positron emission tomography-computed tomography; VIDE, vindesine, ifosfamide, doxorubicin, etoposide; TTE, transthoracic echocardiography.

survived. In addition, CT was biased toward the diagnosis of metastasis in the second case, while its influence on the first case was important.

Although micrometastases cannot be detected on imaging, the inflammatory characteristics around micrometastases can be detected. However, imaging cannot determine the cause of the inflammation, which relies on a combination of clinical and pathological examination. For the first case, if a needle biopsy of inflammatory lesions in the liver or lung had been attempted, it might have provided a reference for us in the diagnosis. We successfully performed puncture biopsies of the abdominal, pleural, and right thigh mass for the second case and obtained the pathological results of the tumor. It has become a consensus that pathological results can be obtained through a biopsy of the metastases. EMB can provide important information for cardiac tumors. The development of related technologies that can directly conduct biopsies of cardiac tumors is a future research direction (8).

In the diagnosis of cardiac tumors, attention should be paid to the application of cardiac imaging. As a basic diagnostic tool, echocardiography can determine the location, number, and size of cardiac tumors; assess cardiac contractility and valve function; and provide information on tumor activity and hemodynamic effects (9). TEE is of great help in the diagnosis of atrial appendage tumors and is also helpful for the development of preoperative planning and intraoperative localization. CE can be used to determine whether the blood supply inside the tumor is rich. Tumors within the heart are often not discovered when a chest scan is performed with MRI or CT. In case 2, chest CT and MRI scans were performed during the first hospitalization, but no tumor was discovered within the heart. It is not uncommon to find a patient with tumor metastasis or recurrence during follow-up, even if no metastatic lesions can be found in preoperative imaging. When a cardiac tumor is suspected to be malignant, PET-CT is a good choice to observe the presence or absence of distant metastases (10).

The prognosis of cardiac malignancy is poor, the median survival for patients with highly malignant PCT is usually 6 to 12 months, and the average survival of patients with PCT undergoing surgical resection varies from 11 to 26 months based on the different degrees of tumor progression and surgical resection ranges (2). One possible reason for this may be that micrometastases or early metastases already exist before surgical excision, resulting in postoperative recurrence. Although it is difficult to confirm metastasis on imaging or obtain tumor tissue for pathological examination by needle biopsy, the inflammatory features of micrometastases or early metastases may suggest the presence of metastases, especially in cases of refractory pneumonia.

Conclusions

Unexplained refractory pneumonia may be a sign of micrometastases from cardiac malignancy. Although micrometastases cannot be detected on imaging, the inflammatory signs around metastases can be detected. When pneumonia is severe and refractory, the presence micrometastases should be considered. At this time, surgery to remove intracardiac tumors requires careful

deliberation.

Acknowledgments

The authors would like to thank Liantu He of the First Affiliated Hospital of Guangzhou Medical University for her help during the follow-up of cases and Qiaoqiong Chen of Dongguan People's Hospital of Southern Medical University for her help in the process of case data collation. *Funding:* The study was supported by the Department of Science and Technology of Guangzhou (No. 202201020424), the First Affiliated Hospital of Guangzhou Medical University (No. ZH202104), and the Guangzhou Medical University Undergraduate Innovation Ability Enhancement Program.

Footnote

Conflicts of Interest: All authors have completed the ICMJE uniform disclosure form (available at https://qims.amegroups.com/article/view/10.21037/qims-22-1002/coif). The authors have no conflicts of interest to declare.

Ethical Statement: The authors are accountable for all aspects of the work in ensuring that questions related to the accuracy or integrity of any part of the work are appropriately investigated and resolved. All procedures performed in this study were in accordance with the ethical standards of the institutional and/or national research committee(s) and with the Helsinki Declaration (as revised in 2013). Written informed consent was obtained from the patient or the patient's parents to publish this case report and accompanying images. A copy of the written consent is available for review by the editorial office of this journal.

References

1. Linfeng Q, Xingjie X, Henry D, Zhedong W, Hongfei X, Haige Z. Cardiac angiosarcoma: A case report and review of current treatment. Medicine (Baltimore) 2019;98:e18193.
2. González LR, Toloza AC, Reyes MR, Spencer LL, Seguel SE, Stockins LA, Jadue TA, Riquelme UA, Ávalos TM, Barra MS, Alarcón OF, Alarcón CE. Primary cardiac tumors. Experience in 72 cases. Rev Med Chil 2020;148:327-35.
3. Look Hong NJ, Pandalai PK, Hornick JL, Shekar PS, Harmon DC, Chen YL, Butrynski JE, Baldini EH, Raut CP. Cardiac angiosarcoma management and outcomes: 20-year single-institution experience. Ann Surg Oncol 2012;19:2707-15.
4. Grankvist R, Chireh A, Sandell M, Mukarram AK, Jaff N, Berggren I, Persson H, Linde C, Arnberg F, Lundberg J, Ugander M, La Manno G, Jonsson S, Daub CO, Holmin S. Myocardial micro-biopsy procedure for molecular characterization with increased precision and reduced trauma. Sci Rep 2020;10:8029.
5. Roe K. An inflammation classification system using cytokine parameters. Scand J Immunol 2021;93:e12970.
6. Mantovani A, Allavena P, Sica A, Balkwill F. Cancer-related inflammation. Nature 2008;454:436-44.
7. DiGiacomo JW, Gilkes DM. Tumor Hypoxia As an Enhancer of Inflammation-Mediated Metastasis: Emerging Therapeutic Strategies. Target Oncol 2018;13:157-73.
8. Ding SW, Tang Q, Zhou DZ, Zhang YM, Zhou XH, Sun T. A device for biopsy of cardiac tumor tissue. CN202120014281.1.
9. Morka A, Kohut J, Radzymińska-Chruściel B, Mroczek T, Gładki M, Weryński P, Rudziński A, Skalski J, Szydłowski L. Echocardiography and Newer Imaging Techniques in Diagnosis and Long-Term Follow-Up of Primary Heart Tumors in Children. Int J Environ Res Public Health 2020;17:5471.
10. Meng J, Zhao H, Liu Y, Chen D, Hacker M, Wei Y, Li X, Zhang X, Kreissl MC. Assessment of cardiac tumors by (18)F-FDG PET/CT imaging: Histological correlation and clinical outcomes. J Nucl Cardiol 2021;28:2233-43.

Cite this article as: Ding S, Chen J, Huang X, Zheng C, Sun T, Wu Z, Qin J. Preoperative considerations of inflammation and metastasis in cardiac malignancies: a description of two cases. Quant Imaging Med Surg 2023;13(5):3357-3364. doi: 10.21037/qims-22-1002

